J Fluoresc (2011) 21:1485–1497
DOI 10.1007/s10895-011-0835-1

ORIGINAL PAPER

Azonium-Ammonium Tautomerism and Inclusion Complexation of 1-(2,4-diamino phenylazo) Naphthalene and 4-aminoazobenzene

G. Venkatesh · A. Antony Muthu Prabhu · N. Rajendiran

Received: 1 August 2010 / Accepted: 10 January 2011 / Published online: 1 February 2011

Abstract Spectral characteristics of 1-(2,4-diamino phenylazo) naphthalene (FBRR, fat brown RR) and 4-aminoazobenzene (AAB) have been studied in various solvents, varying hydrogen ion concentrations and in β-cyclodextrin (β-CD). The inclusion complex of FBRR and AAB with β-CD were analysed by UV-visible, fluorometry and CAche-DFT methods. Solvent study reveals that only azo tautomer is present in both compounds and the large red shifted absorption and emission maxima of FBRR indicate naphthalene ring effectively increases the π-π* transition. Unusual red shift is observed in acid solutions suggests azonium-ammonium tautomer is present in both molecules. In β-CD solutions, the large hypsochromic shift is observed in S_0 and S_1 states indicates *ortho* amino group of FBRR molecule is entrapped in the β-CD cavity and the large bathochromic shift for AAB in the S_1 state indicates 1:1 inclusion complex is formed.

Keywords Fat brown RR · Tautomerism · β-cyclodextrin · Inclusion complex · Solvent · pH effect

Introduction

One-dimensional supramolecular aggregates with well-defined structures assembled from cyclodextrin-based building blocks, such as rotaxenes/catenanes [1–4], molecular shuttles [5], molecular tubes [6], and missing links [7] etc., are currently of much interest in chemistry and materials science. A generally accepted reason for choosing cyclodextrins (CDs), a class of cyclic oligosaccharides with 6–8 D-glucose units linked by α-1,4-glucose bonds, as the starting materials to construct the supramolecular architectures is that the truncated cone-shaped hydrophobic cavities of CDs have a remarkable ability to include various guest molecules either in solution or in the solid state to form the functional host-guest inclusion complexes [8–11], which can be subsequently used as the building blocks of supramolecular aggregates. Among the various families of organic compounds used as guest molecules, the chromophoric guests, such as anthracenes [12], pyrenes [13], and azobenzenes [15–18], are of particular importance because they can exhibit appreciable spectral changes upon inclusion complexation with CDs in solution and thus can be applied as the versatile spectral probes to investigate host-guest complexation.

In the past three decades, a number of CD studies on the host-guest inclusion complexes of CDs with guest molecules have been performed to obtain direct evidence for the formation of the inclusion complexes [19–22]. The obtained results indicate that the structure of these CD inclusion complexes is designable by appropriately selecting the type, length, functional substituent group and heteroatom in the guest. However, comparative studies on the inclusion complexation and assembly behaviour of CDs with azo derivatives are still rare, to the best of our knowledge, although azo derivatives are widely focused upon their potential to construct photo-driven molecular machines [5, 14]. Liu et al. reported on the binding ability and assembly behavior of β-CD with 4-hydroxyazobenzene (HAB) and 4-aminoazobenzene (AAB) in both solution and the solid state [22], which indicted that the disparity of nitrogen atom's position in azobenzene leads not only to distinct crystal systems and space groups, but also to different binding modes and thermodynamic parameters upon complexation with β-CD in aqueous solution [23, 24].

G. Venkatesh · A. A. M. Prabhu · N. Rajendiran (✉)
Department of Chemistry, Annamalai University,
Annamalai Nagar 608 002 Tamilnadu, India
e-mail: drrajendiran@rediffmail.com

In this regard, we report the formation of two self-assembled supramolcular aggregates from 1-(2,4-diamino-phenylazo) naphthalene (or) 4-naphthalen-1-yl diazenyl benzene-1,3-diamine (FBRR, fat brown RR) and AAB (Fig. 1) complexes by extensive hydrogen bond and π-π* interactions. A special interest of these aggregates is their linear or wave-type array achieved by slightly tuning the substituents of the azobenzene derivatives, which will provide an efficient method to control the inclusion and packing mode of supramolcular self-assemblies based on the molecular recognition mechanism. Moreover, the present investigation helped us to understand how and to what extent the disparity of substituents affected the inclusion complexation and assembly behaviour of azobenzene guests with CDs.

In the present study, we have selected FBRR and AAB with the following points in mind: (1) whether the presence of naphthalene ring (a) affect the spectral characteristics of FBRR and AAB (b) will favour the azo-ammonium tautomer in the solvents and β-CD (2) how the presence of *ortho* amino group affect the conjugation (3) whether or not the prototropic reactions of the respective basic or acidic centre are affected by the presence of naphthalene ring and *ortho* amino group and (4) whether the inclusion complexes of both molecules follows similar trend or not. Thus the spectral characteristics of both molecules have been studied in solvents of different polarity, pH and β-CD both in the S_0 and S_1 states and discussed.

Experimental

FBRR, AAB and β-CD were obtained from Sigma-Aldrich and used as such. The purity of the compounds was checked by similar fluorescence spectra when excited with different wavelengths. All solvents used were of the highest grade (Spectrograde) commercially available. Triply distilled water was used for the preparation of aqueous solutions. Solutions in the pH range 2.0–12.0 were prepared with appropriate amounts of NaOH and H_3PO_4. A modified Hammett's acidity

Fig. 1 CAche-DFT structure of FBRR and AAB

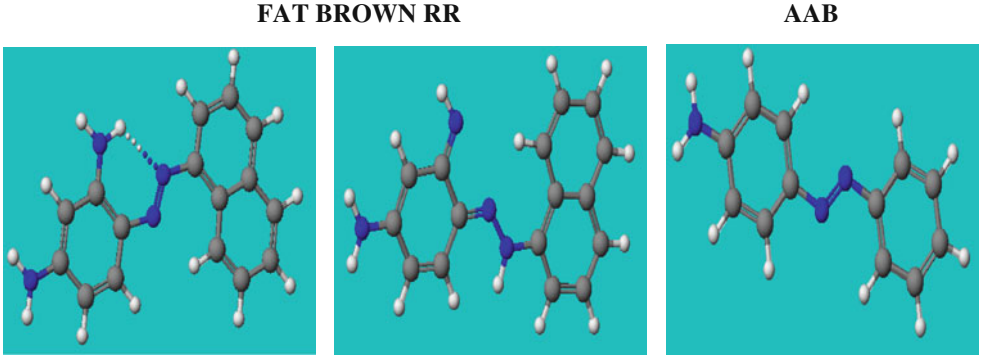

FBRR Bond distance (Å)

ΔH: azo = 118.71302 kcal ammonium = 146.4460 kcal/mol

Dipole moment: azo = 3.049 ammonium = 4.732

H_3-H_{11} = 12.29	H_{11}-H_{13}= 4.76	H_3-N_2 = 6.19	H_4-H_{10}= 12.32
H_{10}-H_{14} = 6.56	H_4-N_2 = 6.40	N_1-H_{11}= 6.94	H_2-H_5 = 6.76
H_5-N_2 = 6.32	N_1-H_{10} = 7.10	H_1-H_6 = 6.83	N_1-H_{14}= 2.25
H_{13}-H_8 = 5.47	H_{14}-H_8 = 4.85		

AAB Bond distance (Å)

ΔH: azo = 97.9517 kcal/mol ammonium = 123.1073 kcal/mol

Dipole moment: azo = 2.251 ammonium = 3.696

H_1–H_8 =12.244	N_3–N_1 =6.415	H_1–N_1 =11.717	N_2–N_1 =5.654
C_1–C_7 =3.639	N_1–H_8 =0.994	C_1–N_1 =7.822	N=N =1.232
C_4–N_1 =10.621	N_2–C_7 =1.437	C_7–N_1 =4.227	N_3–C_1 =1.431
C_{10}–N_1 =1.392			

scale [25] (H_0) used for the solutions below pH ~2 (using a H_2SO_4-H_2O mixture) and Yagil's basicity scale (H_-) [26] used for solutions above pH ~12 (using a NaOH-H_2O mixture) were employed. The solutions were prepared just before each measurement. The concentration of the FBRR/AAB solutions was of the order of 2×10^{-5} M and that of β-CD solution was varied from 1×10^{-3} M to 1×10^{-2} M.

Absorption spectral measurements were carried out with a Hitachi (model U-2001) UV-visible spectrophotometer and fluorescence measurements were made with a Shimadzu RF-5301 spectrofluorometer. The pH values in the range 2.0–12.0 were measured on an Elico pH meter (model LI-120).

Results and Discussion

Effect of Solvents

The absorption maxima, molar extinction coefficient, emission maxima and Stokes shifts of FBRR and AAB were studied in different solvents and the relevant data are complied in Table 1. In all solvents the absorption and emission spectral maxima of FBRR is largely red shifted than that of AAB. The results in Table 1 reveal that the presence of naphthalene ring effectively increases the π-π^* transition. In all solvents, similar to that of azobenzene (AB) the absorption bands of both amino compounds consisted of two peaks (FBRR: cyclohexane, λ_{abs}~420, 290 nm, λ_{flu}~500 nm, methanol, λ_{abs}~448, 290 nm, λ_{flu}~562 nm; AAB: cyclohexane, λ_{abs}~369, 246 nm, λ_{flu}~420 nm, methanol, λ_{abs}~383, 246 nm, λ_{flu}~430 nm). In AB, from cyclohexane to water, the longer wavelength band (LW) was slightly red shifted whereas the shorter wavelength (SW) band was largely red shifted (cyclohexane, λ_{abs}~314, 218 nm, λ_{flu}~370 nm, methanol, λ_{abs}~318, 228 nm, λ_{flu}~362 nm). On the other hand, in FBRR and AAB, the LW band is largely red shifted than SW band (difference in FBRR: ~106 nm in cyclohexane and ~141 nm in methanol; difference in AAB: ~55 nm in cyclohexane and ~63 nm in methanol). In water, red shifted absorption

Table 1 Absorption and fluorescence spectral data (nm) observed for FBRR and AAB in different solvents

Solvents	FBRR				AAB			
	λ_{abs}	log ε	λ_{flu}	Stokes shift	λ_{abs}	log ε	λ_{flu}	Stokes shift
Cyclohexane	420	4.44	500	3,810	369	4.41	420	3,571
	290s	4.40			246	4.20		
	271	4.22						
	246s	4.26						
	212	4.90						
1,4-Dioxane	447	4.43	510	2,763	384	4.41	426	2,567
	290s	4.24			249	4.20		
	269	4.20						
	246s	4.28						
Acetonitrile	447	4.53	559	4,482	384	4.41	429	2,731
	290s	4.00			250	4.20		
	269	4.42						
	246s	4.38						
	211	4.91						
2-Propanol	450	4.46	560	4,365	384	4.41	430	2,786
	290s	4.06			249	4.20		
	266	4.46						
	244s	4.38						
	213	4.91						
Methanol	448	4.51	562	4,527	383	4.41	430	2,786
	290s	4.02			246	4.20		
	268	4.44						
	231s	4.38						
	212	4.92						
Water (pH=6.5)	449	4.21	564	4,541	380	4.41	430	3,060
	270	3.88			245	4.20		
	211	4.77						
Correlation coefficient								
$\Delta\bar{\nu}_{ss}$ *vs.* $E_{T}(30)$				0.9192				0.9314
$\Delta\bar{\nu}_{ss}$ *vs.* BK				0.7496				0.8571

maximum is observed for AB, while a blue shifted absorption maximum is seen for FBRR and AAB. This indicates that the position of both bands are relatively influenced by the changing the solvents.

In all the solvents, the fluorescence spectra of FBRR and AAB molecules show a single emission (Fig. 2). The emission spectrum of FBRR is excited at 400 nm whereas AAB is excited at 370 nm. In FBRR, the emission maximum appears at around 500–550 nm whereas for AAB it is seen at 420–430 nm. Similar to the absorption maxima, the fluorescence maxima of FBRR is more red shifted as compared to that of AAB and AB molecules. Examination of these results reveals that the position and/or the molar extinction coefficient of these bands are highly influenced by the nature of substituent group. Comparing absorption and fluorescence spectral shifts of both compounds indicates that the interaction of naphthalene ring with azo group is more than that of phenyl ring. The shift in the LW band can be assigned to π-π^* transition involving the whole electronic system of the compounds with a considerable charge transfer (CT) character. Such a CT originates mainly from the aromatic ring or amino group to the azo group which is characterized by a high electron accepting character. Due to the greater charge transfer effect of the NH_2 group with the aromatic ring, a larger red shifted maximum is observed in FBRR/AAB than in AB.

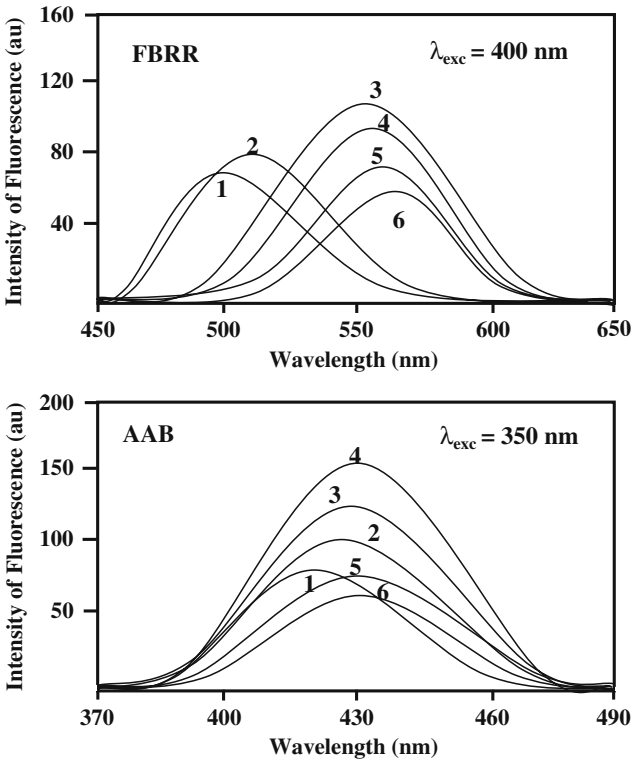

Fig. 2 Fluorescence spectra of FBRR and AAB in selected solvents at 303 K: 1. cyclohexane, 2. dioxane, 3. acetonitrile, 4. 2-propanol, 5. methanol, 6. water

In contrast to azonaphthols, azoanilines and azophenols compounds do not exist as a tautomer mixture in solution at room temperature, e.g., azonaphthol molecules are present in both azo (A) and hydrazo form (H) and their relative stability depends on the solvent and/or temperature [27–33]. The tautomeric behaviour of azonaphthol compounds differ considerably from that of the corresponding azophenols and azoanilines [27] even in polar solvents which exist mainly in azo form at room temperature. Such a difference was be caused by the loss of aromaticity on going from azo to hydrazo form, while in azonaphthol compounds, this effect is compensated by the transfer of aromaticity within the naphthalene fragment; i.e. in FBRR/AAB, the number of delocalized electrons in the tautomeric phenyl ring is reduced from six to four in the H-form. This is because two of these electrons are engaged in the strong C=N and C=O bonds and thus, the phenyl ring looses much of its aromaticity. In naphthol compounds this effect is compensated by the second aromatic ring [34]. Therefore, the above results suggest in all solvents both molecules exhibits only azo form.

Correlation of Solvent Shifts with Solvent Polarity Parameters

When a solute is placed in a solvent, the combined effects of general and specific interactions are observed and the separation of these interactions is often difficult. Empirically or theoretically derived solvent parameters like Reichardt's-Dimroth, $E_T(30)$ [35], Biolet-Kawaski, BK [36] and Lippert *f*(D, n) [37] values as accurate registers of solvent polarity have been used by several authors to correlate molecular spectroscopic properties. Among these parameters BK and *f*(D, n) takes into account the solvent polarity alone, whereas $E_T(30)$ incorporates both solvent polarity and hydrogen bonding effects. A correlation of Stokes shift with any one of these parameters gives an idea about the type of interaction between the solute and solvent.

The correlation of Stokes shifts ($\Delta\nu_{ss}\ cm^{-1} = \overline{\nu}_{abs}\ max - \overline{\nu}_{flu}\ max$) of FBRR, AAB and AB in different solvents with E_T (30) and BK is shown in Fig. 3. The increase in Stokes shift from cyclohexane to water is found to be more in accordance with the $E_T(30)$ than with BK values (Table 1). Since hydrogen bonding interactions are predominant in the solvatochromic shifts.

Effects of pH

The absorption and fluorescence spectra of FBRR and AAB were measured in the pH range H_0 −10 to H– 17 and the spectral maxima are listed in Table 2. Figure 4 illustrates the absorption and fluorescence spectra of various prototropic species of the above molecules. The

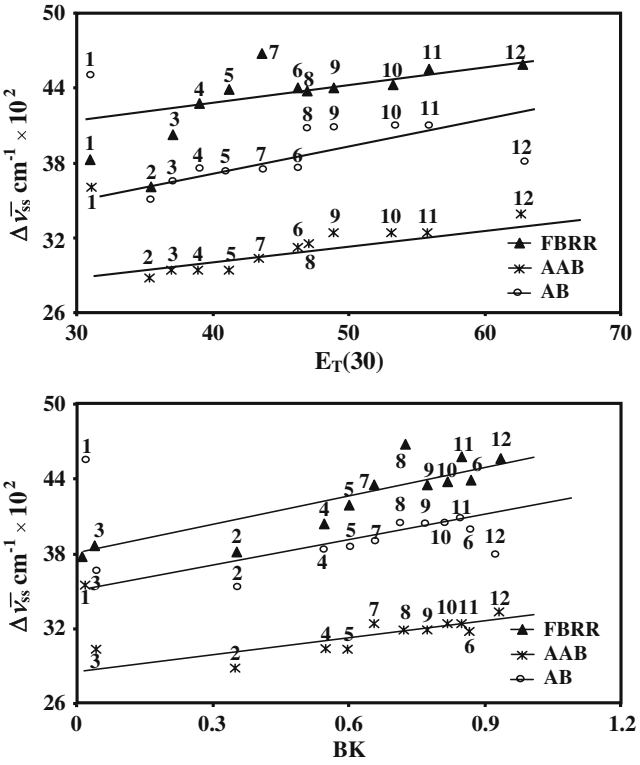

Fig. 3 Plot of Stokes shifts (cm^{-1}) of FBRR, AAB and AB *vs.* $E_T(30)$ and BK solvent parameter: 1. cyclohexane, 2. diethyl ether, 3. 1, 4-dioxane, 4. ethylacetate, 5. dichloromethane, 6. acetonitirle, 7. *t*-butyl alcohol, 8. 2-butanol, 9. 2-propanol, 10. ethanol, 11. methanol, 12. water

effect of proton concentration on the absorption and fluorescence spectra of both the molecules is different to that observed for other aromatic amines [38–40]. When the pH is decreased from 7 to H_0 −1, no significant spectral shift is observed in AB (λ_{abs}~317, 228 nm, λ_{flu}~370 nm), whereas with increasing acid concentrations from H_0 −2, a large red shifted spectrum is observed in both S_0 and S_1 states (λ_{abs}~415, 293sh, 250 nm, λ_{flu}~430 nm) indicating that protonation takes place in the azo group of this molecule. Even at very high acid concentrations (H_0 −10), no further spectral change is noticed in AB molecule indicating dication is not formed in this case.

In both S_0 and S_1 states, the protonation spectral shifts of FBRR and AAB molecules follow a different trend in acid and base environment. The absorbance and emission maxima are regularly red shifted on increasing the acid concentration from pH~7 to H_0~1, suggesting that protonation takes place in the azo group and proton (azonium-ammonium) tautomerism is present in both molecules. This assumption is based on the following reasons: (a) it is well known that if protonation takes place in the amino group, a blue shifted spectrum should be noticed and (b) the absorption maximum of amino molecule (AAB) should resemble with parent (AB) molecule because the protonation will block the amino group lone pair electrons. In both compounds, further increase in the acidity leads to a second protonation although the first process is not fully complete. The absorption and fluorescence maxima of FBRR is largely blue shifted on further increase in the acid concentrations, while large blue shift is observed in AAB indicating the formation of dication i.e.; the second protonation occurs in the NH_2 group [38–40]. This is further confirmed by the resemblance of the fluorescence behaviour of the latter species to that of AB molecule. With an increase in the pH from 11 to 14 newly red shifted absorption spectrum is observed in both amino compounds indicating formation of a monoanion; i.e. deprotonation takes place in the amino group. When the basicity is increased from pH~12, the emission intensity is quenched indicating formation of a non-fluorescent monoanion.

Table 2 Various absorption and fluorescence prototropic maxima of FBRR and AAB in aqueous and β-CD medium

Species	FBRR				AAB			
	Aqueous medium		β-CD medium		Aqueous medium		β-CD medium	
	λ_{abs}	λ_{flu}	λ_{abs}	λ_{flu}	λ_{abs}	λ_{flu}	λ_{abs}	λ_{flu}
Dication	403	430			426	435		
	279	335			215			
	216							
Monocation	465	570	465	460	505	515	480	510
	347	460	360	335	320		224	
	275	335	275		230			
	212		212					
Neutral	448	564	420	460	380	430	384	450
	268	460	260	335	245		252	
	211	334	218					
Monoanion	536	q			395	q		
	285				215			
	228							

q quenching

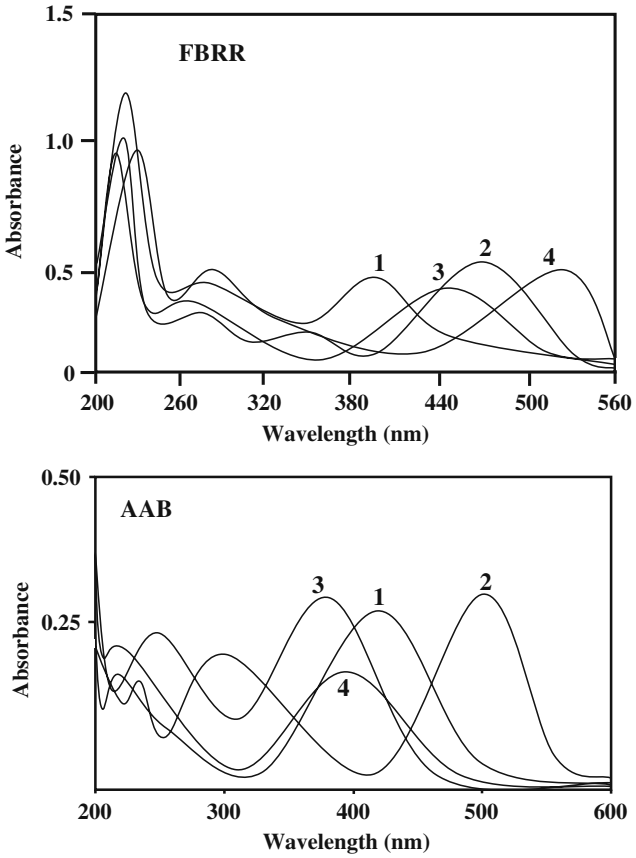

Fig. 4 Absorption spectra of different prototropic species of FBRR and AAB at 303 K: concentration 2×10^{-5} M: (1) dication, (2) monocation, (3) neutral, and (4) monoanion

In acid pH solutions, three absorption spectral maxima are observed for FBRR/AAB (Table 2). The various forms unprotonated (B-band, neutral), monoprotonated (C-band, azonium) and diprotonated (A-band, ammonium) structures are shown in Figs. 5 and 6. Even though, the tautomeric equilibrium depends on acid concentration [41], the influence of the environment (solvent polarity) effects in the investigated compounds maybe explained with the charge transfer (CT) model (Fig. 7), where the amino substituted azobenzene chromophore is classified as a donor (D), acceptor (A) system [28–34]. The azonium structure can be presented with the CT-model by system 2 (Fig. 7). The donor fragment acts in CT model 1 and in the azonium system act as an acceptor in CT model 2; i.e., structural changes in this system result in different effects in the adsorption bands of each configuration.

Based on the above results, it maybe conclude that on protonation, there exist a tautomeric equilibrium between the ammonium (AM) and azonium (AZ) form [28–34, 41] thus the C-band at 465 nm in FBRR and 505 nm in AAB is assigned to the azonium cation, in which the β–azo nitrogen atom is protonated, which is responsible for the large red shift. Also the A-band at 347 nm in FBRR and 320 nm in AAB is associated with the protonated terminal nitrogen of the NH_2 group (ammonium form) and this protonation prevents mesomeric interaction of the terminal lone pair with the π–electronic system.

It is worth noting that the donor fragment in the azo form (CT-model 1) act as an acceptor in the azonium system (CT-model 2), which explains how the structural changes in a particular fragment can lead to different effects in the absorption bands. The introduction of a stronger electron donor (NH_2) substituent instead of hydrogen atom into the AB molecule (unprotonated AAB) causes a bathochromic shift (320–380 nm) of about 60 nm, whereas the introduction of the naphthalene ring (i.e. FBRR) leads to larger red shift (320–449 nm) in the spectral maxima, in accordance with CT model 2. The position of the A-band at 320–330 nm (AAB) associated with the ammonium tautomeric form closely corresponds with that of the compound without a protonated amino group. The C-band of the azonium tautomeric form also has vibronic structure (Fig. 4) and the electronic transition is associated with a charge transfer from the anilino fragment (D) to the quinoniemine fragment (A). It is also of interest to note that the adsorption spectra show the protonation of FBRR/AAB compounds proceeds with relative increase of ammonium and azonium forms.

The protonation of the amino nitrogen by removing the π-electrons of nitrogen from the aromatic resonance system should result in a dicationic species (2) which is iso π-electronic with the protonated azobenzene cation. The absorbance of the AB monocation (424 nm) is in fact very close to the absorption of the observed diprotonated species (426 nm in AAB). This is taken as an evidence for the second conjugate acid of FBRR having structure 2 (Fig. 8).

There is also a possibility that a second protonation occurs on the azo group, to give structure 2 (Fig. 8).

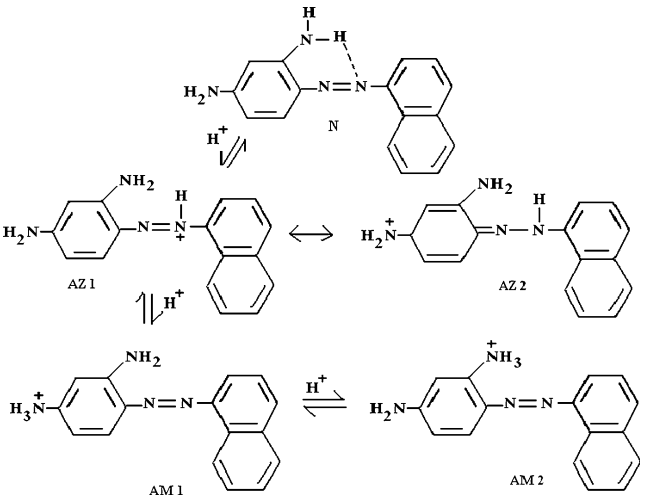

Fig. 5 Various protonated form of FBRR

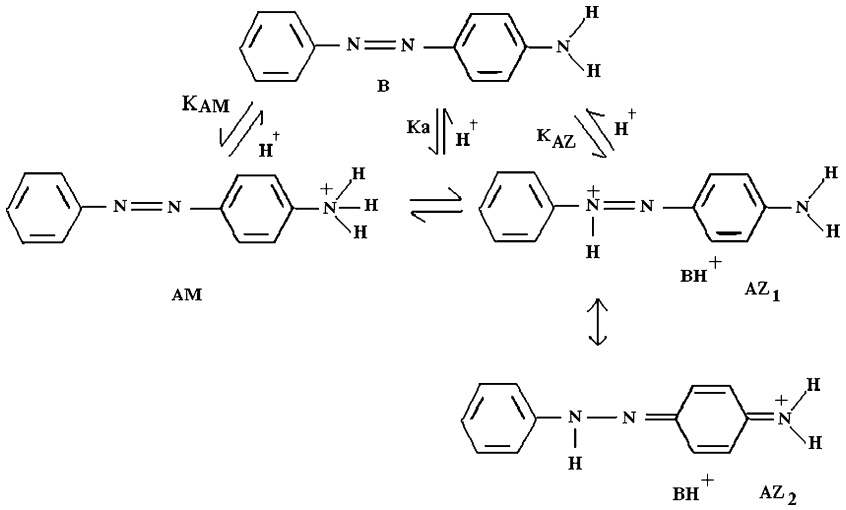

Fig. 6 Various protonated form of AAB

However in that case, structure 2 should be an important contributor by analogy with monoprotonated FBRR/AAB. Consequently, one would expect the diprotonated FBRR/AAB to have its absorption maximum largely unchanged from the monoprotonated form, which is not the case herein. A noteworthy point is that azobenzene itself apparently does not undergo a second protonation even in 100% H_2S0_4, which suggests that protonation of both nitrogen in the azo group is relatively unfavorable. In order to obtain pK_a values for all the corresponding equilibrium (i.e. dication-monocation, monocation-neutral, neutral-monoanion), the absorbance and emission intensity data when plotted against H_0/pH/H_ give typical sigmoid curve is obtained. From the inflexion point, the pK_a (dication–monocation, monocation-neutral) values of −3.6 and 0.8 are obtained respectively (Table 3).

Effects with β-CD

Table 4, Figs. 9 and 10 depicts the absorption and emission spectra of FBRR, AAB and AB in pH ~7 aqueous solutions containing different concentrations of β-CD were recorded. With an increase of β-CD concentrations, the absorption maxima of FBRR were regularly blue shifted from water to 10×10^{-3} M β–CD concentration (λ_{abs}~448 nm–418 nm) whereas no spectral shift is observed in AAB (λ_{abs}~380 nm) and AB (λ_{abs}~317 nm). The molar extinction coefficients of these molecules are increases along with increase in β-CD concentrations and the measured absorbance is plotted against [β-CD] (inset Fig. 9). The above results indicate that these molecules are entrapped in the β-CD cavity to form inclusion complex. The absorbance of the solutions recorded after 12 h remains constant revealing the fact that the above molecules present in β-CD solution without decomposing on keeping and this is due to the formation of inclusion complex. This behavior may be attributed to the enhanced dissolution of the guest molecule through the hydrophobic interaction [42–45] between guest and non-polar cavity of β-CD.

The fluorescence characteristics of FBRR and AAB undergo drastic changes in the presence of β-CD (Fig. 10). As the β-CD concentration is increased, the fluorescence intensity of AB (370 nm) increases significantly at the same emission wavelength whereas in AAB the fluorescence maximum is red shifted (430 nm–455 nm) and the emission intensity increases along with β-CD concentration. Interestingly, upon increasing the β-CD concentrations the longer wavelength emission of FBRR is largely blue shifted from 560 nm to 459 nm and the fluorescence intensity is decreased in 560 nm whereas it is increased at 459 nm. Such changes in both molecules caused by the introduction of β-CD are indicative of the formation of an inclusion complex. The difference in the results between FBRR and AAB implies that the inclusion process for both molecules

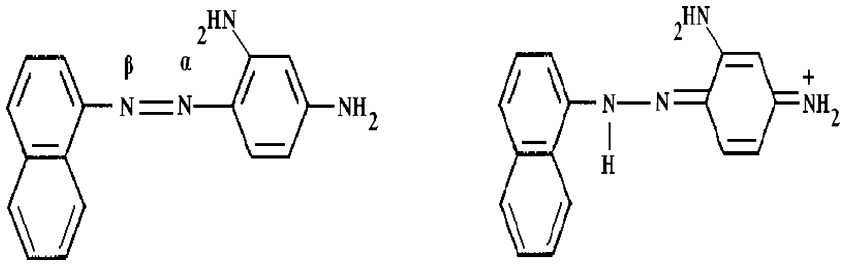

Fig. 7 CT Model 1 and CT Model 2

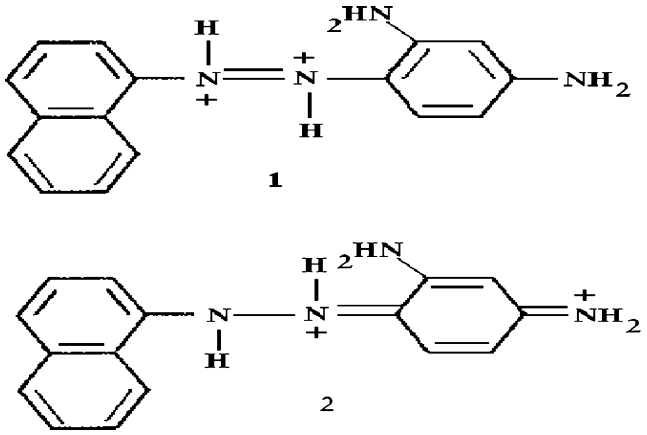

Fig. 8 Diprotonated species of FBRR

is different. The considerable increase in the fluorescence intensity compared with absorbance means that the quantum yields of both azo molecules increase in the presence of β-CD.

The presence of isosbestic points in these compounds indicates 1:1 inclusion complex is formed. In general, the existence of an isosbestic point in the absorption spectra is indicative of the formation of well defined 1:1 complex [46–50]. The formation constant of AAB is small compared than that of FBRR with β-CD. This is probably AAB molecule is not tightly encapsulated into the cavity, whereas due to presence of naphthalene ring and *ortho* amino group in the phenyl group in FBRR, this molecule may tightly encapsulate in the β-CD cavity.

For 1:1 complex between β-CD and guest molecule (FBRR, AAB and AB) the following equilibrium can be written:

$$\mathrm{FBRR} + \beta - \mathrm{CD} \;\rightleftharpoons\; \mathrm{FBRR}\ldots.\beta - \mathrm{CD} \qquad (1)$$

The formation constant 'K' and stoichiometric ratios of the inclusion complex of the above compounds were determined according to the Benesi-Hildebrand relationship [51] assuming the formation of a 1:1 host-guest complex:

$$\frac{1}{I - I_0} = \frac{1}{I' - I_0} + \frac{1}{K(I' - I_0)[\beta - CD]_0} \qquad (2)$$

where $[\beta\text{-CD}]_0$ represents the initial concentration of β-CD, I_0 and I are the absorbance and fluorescence intensities in the absence and presence of β-CD respectively and I′ is the limiting intensity of absorbance and fluorescence. The 'K' values were obtained from the slope and the intercept of the plots (Figs. 11 and 12). The Benesi-Hildebrand plot shows excellent linear regression supporting the formation of the 1:1 inclusion complex.

The free energy change of these complex were calculated from the following equation

$$\Delta G = -RT \ln K \qquad (3)$$

The value of ΔG is negative (Table 4), which suggests that the inclusion process proceeds simultaneously at 303 K. The negative value in the experimental temperature indicates that the inclusion process is an exothermic and enthalpy controlled process. The hydrophobic interaction between the internal wall of β-CD and guest molecules is an important factor for the stability of inclusion complexes [52]. In FBRR and AAB, it may safely be considered that the difference in the magnitude of the hydrophobic interaction is related to that of the contact area of the guest molecule for the internal wall of β-CD.

Several driving forces have been postulated for the inclusion complexation of CD with guest compounds [53]: (1) van der Waals forces, (2) hydrophobic interactions, (3) hydrogen bonding, (4) release of distortional energy of CD by binding guest and (5) extrusion of 'high energy water' from the cavity of CD upon inclusion complex formation. Tabushi [54] proposed a thermodynamic model for the process of CD inclusion complex formation. Based on the thermodynamic parameter (ΔG) calculated for the inclusion of FBRR and AAB, we conclude that the hydrophobic interactions, van der Waals interaction, and breaking of the water cluster around this polar guest compounds mainly dominate the driving force for inclusion complex formation.

It is well known that the strength of interaction is also dependent on the size of the CD cavity and size of the substituent in the complex [55]. This means that the interaction is more sensitive to the size of substituent and the CD in the complexation. The CDs are truncated, right-

Table 3 pK_a (pK_a^*) values of different prototropic equilibrium of FBRR and AAB in the S_0 and S_1 states

Equilibrium	FBRR				AAB			
	Aqueous medium		β-CD medium		Aqueous medium		β- CD medium	
	pK_a abs	pK_a^* FT	pK_a abs	pK_a^* FT	pK_a abs	pK_a^* FT	pK_a abs	pK_a^* FT
Dication monocation	−2.0	−1.9			−3.6	−3.4		
Monocation neutral	3.0	0.8	3.2	0.9	1.1	1.0	0.96	0.84
Neutral monoanion	14.0	15.0			14.5	14.3		

Table 4 Absorption and fluorescence maxima (nm) of FBRR and AAB in different β-CD concentrations

Concentration of β-CD (M)	FBRR			AAB		
	λ_{abs}	log ε	λ_{flu}	λ_{abs}	log ε	λ_{flu}
Water	449	4.21	564	380	4.41	430
	270	3.88		245	4.20	
	211	4.77				
0.001	429	4.29	559	382	4.45	455
	270	3.92		247	4.27	
	213	4.85				
0.002	424	4.30	459	382	4.47	455
	260	3.97		248	4.30	
	214	4.84				
0.004	421	4.36	459	382	4.49	455
	258	4.13		250	4.36	
	217	4.90				
0.006	420	4.43	460	382	4.50	455
	260	4.27		252	4.38	
	218	4.97				
0.008	419	4.45	460	382	4.52	455
	260	4.36		253	4.54	
	218	5.00				
0.010	418	4.49	460	382	4.52	455
	267	4.42		253	4.55	
	218	5.03				
Excitation wavelength	400			370		
Binding constant (K) (M^{-1})	557		813	523		624
ΔG KJ / mole	−15.90		−17.47	−15.87		−16.27

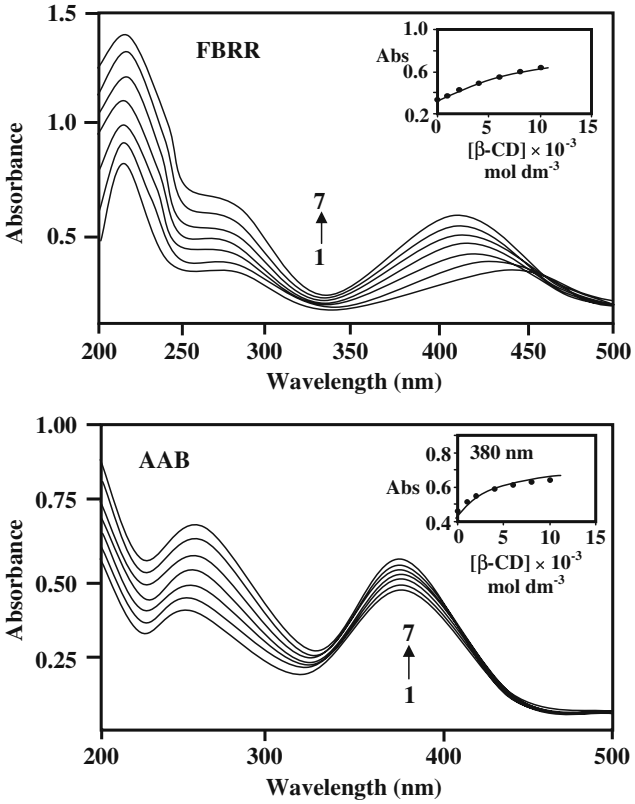

Fig. 9 Absorption spectra of FBRR and AAB in different β-CD concentrations (M): 1. 0, 2. 0.001, 3. 0.002, 4. 0.004, 5. 0.006, 6. 0.008, 7. 0.01

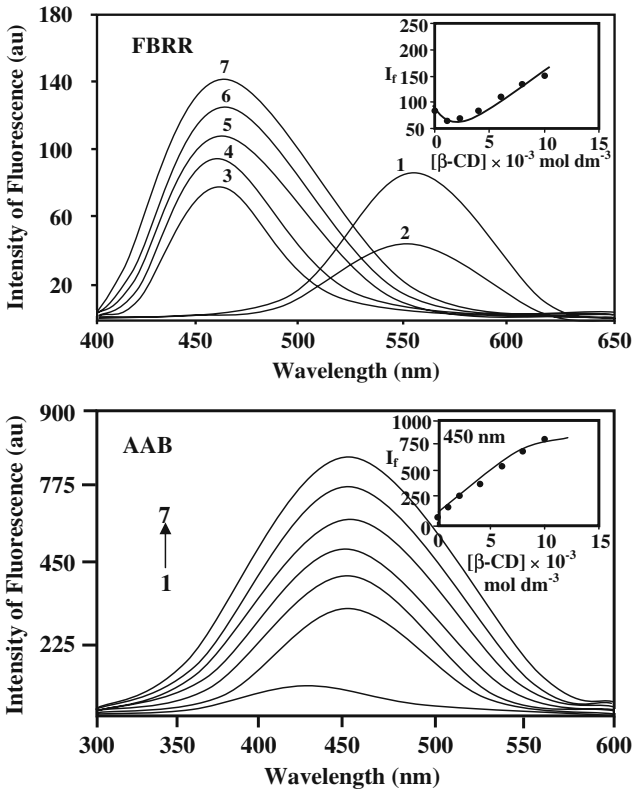

Fig. 10 Fluorescence spectra of FBRR and AAB in different β-CD concentrations (M): 1. 0, 2. 0.001, 3. 0.002, 4. 0.004, 5. 0.006, 6. 0.008, 7. 0.01

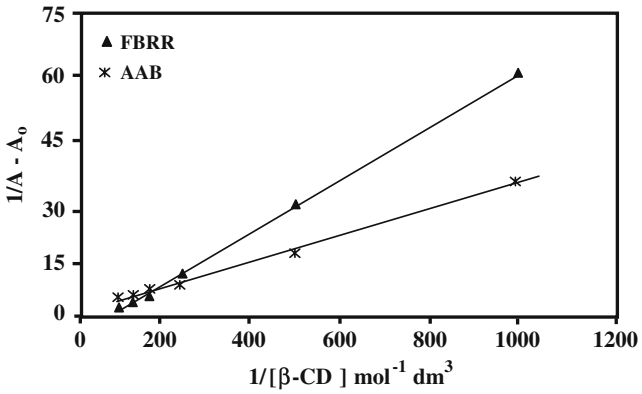

Fig. 11 Absorption spectra of Benesi-Hildebrand plot for the complexation of FBRR, AAB and AB with β-CD (Plot of 1/ΔA *vs.* 1/[β-CD])

cylindrical, cone-shaped molecules, 7.8Å heights with a central cavity. The diameter of the wider and narrower rim of the β-CD cavity was found to be 6.5Å and 5.8Å, respectively [56]. It is well known that the van der Waals force including the dipole–induced dipole interactions [57] are proportional to the distance between the guests and the wall of the CD cavity and to the polarizabilities of the two components. The phenyl moiety may achieve a maximum contact area [58] with the internal surface of the cavity of the β-CD; hence, the interaction of the phenyl ring with β-CD would play an important role.

In general, the inclusion of CDs with guest compounds is also affected by hydrophobic and electronic interactions [57–59]. Since CDs have a permanent dipole [60], the primary hydroxyl end is positive and the secondary hydroxyl end is negative in the glucose units of CDs. The stability of binding by hydrophobic interaction is partly the result of van der Waals force but is mainly due to the effects of entropy produced on the water molecules [61]. In aqueous solution, a hydrophobic guest compound is

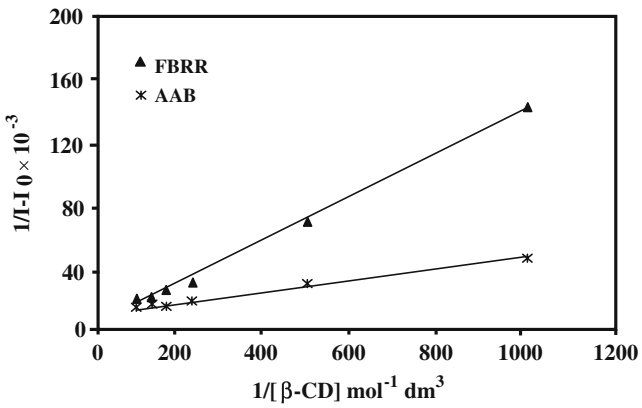

Fig. 12 Fluorescence spectra of Benesi-Hildebrand plot for the complexation of FBRR, AAB and AB with β-CD (Plot of 1/I–I_0 *vs.* 1/[β-CD])

restricted by the water shell formed by the hydrogen bonding network [62]. It has a strong tendency to break down the water cluster and penetrate the apolar cavity of CD. This process is exothermic due to entropic gain [63, 64]. The association constants for the inclusion of β-CD with guest compounds were observed to be proportional to the substituent hydrophobic constant of the guest. In azo molecules, since the amino substituent locates near the wider rim of the CD cavity and phenyl ring locates narrower range of the CD cavity, the 'K' values are proportional to the hydrophobic interactions. The difference in slope in Figs. 11 and 12 for FBRR/AAB and β-CD complexes indicates that the hydrophobic interactions with β-CD are much stronger than hydrogen bonding interactions because FBRR/AAB interaction is approximate to the hydrophobic contact (Table 1).

From the above results, we notice some interesting points: (a) the 'K' value for FBRR is higher than that of AAB which is attributed to the more hydrophobic interaction between the naphthalene ring and the internal wall of β-CD; (b) the small binding constant for AAB implies that the phenyl ring is not more tightly embedded in the β-CD cavity; (c) in FBRR, the large blue shifted absorption and emission spectra suggests both amino groups are present in the interior part of the β-CD cavity; (d) in AAB, the large red shifted emission spectra suggest amino group is present in the hydrophilic part of the β-CD cavity (Fig. 13). The results in Table 4 conforms the molecular disposition of FBRR in the inclusion complex is different to that of AAB [65]. Further it is a well known fact that hydrophobicity is the driving force for the formation of inclusion complexes. Since naphthalene/phenyl group is more hydrophobic than aniline part the naphthalene/phenyl ring may include in the β-CD cavity. It is also recognized that the amino group is located outside the β-CD cavity (in hydrophilic environments) [42–45].

Possible Inclusion Complex

According to Yu Liu's [66] study on β-CD/azo complexes, we can deduce that both molecules is included longitudinally in the β-CD cavity. The absorption and emission spectrum of FBRR in β-CD solutions are shifted to shorter wavelength (Table 4) suggesting both amino groups are present in the interior part of the β-CD cavity. However, the emission spectrum of AAB in β-CD solutions are shifted to longer wavelength (420–455 nm), this may be due to a higher conjugated system between two benzene rings; i.e. the two benzene rings are located almost in the same plane. Further, like HAB and 4-amino-2′,3-dimethylazobenzene, both molecules (FBRR and AAB) exhibit similar spectral shape and emission maximum around ~455 nm suggesting that both benzene rings are located similarly.

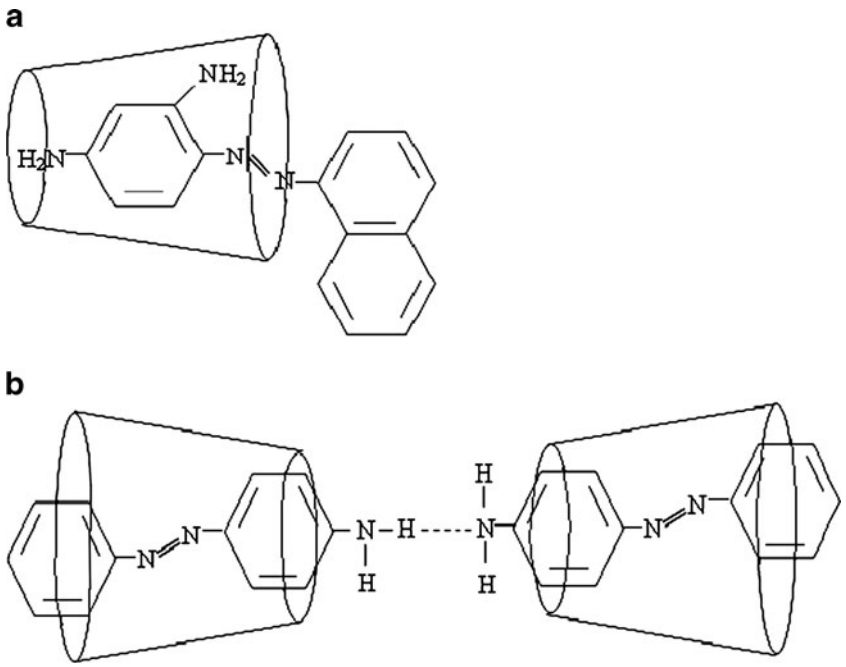

Fig. 13 Proposed inclusion complex structure of (**a**) FBRR and (**b**) AAB

The above results in the β–CD medium are explained as follows: AAB molecule is embedded in β-CD cavity in different directions to form the 1:1 inclusion complex and the amino group of AAB molecule points to the wider side of the β-CD cavity [66]. This is attributed to the cooperative interactions of eight hydrogen bonds between the secondary hydroxyl groups β-CD unit as well as the π-π* interaction between the benzene rings. FBRR/AAB molecules are embedded into the β-CD cavity in different directions with the amino group of the azo molecules pointing to the wider side of the β-CD cavity (1:1 stoichiometry between FBRR/AAB with β-CD are formed).

More interestingly, AAB molecule adopts different orientations of β-CD which consequently result in the formation of longer wavelength emission maxima (Fig. 10). Further, water molecules are located on the exterior part of the β-CD cavity and both benzene rings are included in the β-CD cavity which indicates the presence of stronger hydrophobic interaction between the guests and β-CD cavity. In AAB, the strong hydrogen bond network formed by the -OH groups of the β-CD and amino group of azobenzene further extend the longer wavelength emission. On the other hand, in FBRR, a large hypsochromic shift is observed in the absorption spectra confirmed the *ortho* amino group is encapsulated in the β-CD cavity.

Let us now consider possible type of inclusion complexes also: (i) as like in AB, if 1:1 inclusion complex is formed or azo molecule is partially (i.e. the benzene ring) entrapped in the β-CD cavity. In such a case, this type of complex is formed the emission maxima of FBRR/AAB should increase at the same wavelength and, if other part of azo molecule (i.e. the aniline ring) include with in the β-CD cavity, the monocation maxima in the absorption and emission maxima (i.e. protonation of amino group) should be blue shifted as compared to the aqueous medium [46, 47]. The values of prototropic equilibrium, absorption and emission maxima indicate that neutral maximum is largely blue shifted as compared to the aqueous medium. Monocation maximum also follows similar trend both in aqueous and β-CD medium. It has been reported, that when amino group is entrapped in the β-CD cavity, the neutral/monocation absorption maximum is blue shifted in β-CD as compared to in aqueous medium [46–50]. Further, the large blue shift of the S_0 /S_1 states in FBRR and the large red shift of the S_1 state in AAB, supports the fact that in FBRR the *ortho* amino group is present in the β-CD cavity where as in AAB the amino group is present in a more polar environment than water. The question may arise why the fluorescence intensity of AAB is greatly enhanced along with red shift in β-CD solutions? This may be because viscosity is increased along with β-CD concentrations [43–45] also that in β-CD solutions of higher concentrations, due to viscosity the dimer interaction is increased which greatly enhances the fluorescence intensity along with red shift in AAB and the large blue shift in FBRR reveals that *ortho* amino group is present in the hydrophobic part and the FBRR emission maximum in the β-CD solutions resembles with AAB indicating, in both molecules similar inclusion complex is formed. This confirms that the environment around the *ortho* amino group in β-CD is different from the bulk aqueous medium.

This is further supported by using semi empirical quantum calculations (DFT/CAche 7.5 PC-model program)

which provide some useful information about the inclusion complexation geometry of guest molecules. To determine the dimensions of FBRR and AAB geometry and β-CD, in the ground state were optimized by using the DFT/CAche program. This method provides acceptable approximations to give results, which are quite close to the experimental findings. The internal diameter of the β-CD was found to be approximately 6.65 Å and its height is 7.8 Å (Fig. 13). Considering the shape and dimensions of β-CD, both molecules can not completely get encapsulated with in the β-CD cavity, because in FBRR distance between H_1-H'_8 is 12.290 Å, H_4-H'_{10} is 12.321 Å, N_1-H'_{10} is 7.10 Å, H_2-H'_5 is 6.762 Å and in AAB the distance between H_4-H'_4 is 11.403 Å, H_4-H'_6 is 7.781 Å, H_4-H'_4 is 8.200 Å, C_4-C'_4 is 9.210 Å, C_3-C'_3 is 7.816 Å, C_4-C'_3 is 8.706 Å, H_4-C'_4 is 10.306 Å, H_4-C'_3 is 9.587 Å, H_4-C'_2 is 8.425 Å; these values are greater than the inside diameter of the β-CD cavity (6.65 Å) which may be responsible for the formation of different types of inclusion complexes in the β-CD.

Conclusions

The solvent study reveals only the azo tautomer is present in FBRR and AAB compounds. The large red shifted absorption maximum of FBRR indicating that the naphthalene ring is effective in increasing the spectral behaviour of this molecule. Unusual red shift observed in acid solution suggests that the azonium-ammonium tautomer is present in both the molecules. In β-CD solutions, the increase in the fluorescence intensity and a large blue shift in S_0 and S_1 states indicates that in FBRR *ortho* amino group is entrapped in the β-CD cavity. The increase in the fluorescence intensity and a large bathochromic shift in S_1 state indicate FBRR/AAB forms 1:1 inclusion complex with β-CD.

Acknowledgement This work is supported by the Department of Science and Technology, New Delhi, (Fast Track Proposal-Young Scientist Scheme No. SR/FTP/CS-14/2005) and University Grants Commission, New Delhi (Project No. F-31-98/2005 SR). One of the authors A. Antony Muthu Prabhu is thankful to CSIR, New Delhi for the award of Senior Research Fellowship (SRF).

References

1. Okada M, Harada A (2004) Org Lett 6:361
2. Terao J, Tang A, Michels JJ, Krivokapic A, Anderson HL (2004) Chem Commun 56
3. Look JS, May BL, Clements P, Lincoln SF, Easton CJ (2004) Org Biomol Chem 2:337
4. Liu Y, Zhao YL, Zhang HY, Li XY, Liang P, Zhang XZ, Xu JJ (2004) Macromolecules 37:6362
5. Wang QC, Qu DH, Ren J, Chen K, Tian H (2004) Angew Chem Int Ed 43:2661
6. Saito M, Shimomura T, Okumura Y, Ito J, Hayakawa R (2001) J Chem Phys 114:1
7. Liu Y, Zhao YL, Zhang HY, Song HB (2003) Angew Chem Int Ed 42:3260
8. Szejtli J, Osa T (1996) In: Atwood JL, Daves JE, MacNicol DD, Vogtle F (eds) Comprehensive supramolecular chemistry, vol III. Pergamon/Elsevier, Oxford
9. Liu Y, Wang H, Liang P, Zhang HY (2004) Angew Chem Int Ed 43:2690
10. Mulder A, Jukovic A, Huskens J, Reinhoudt DN (2004) Org Biomol Chem 2:1748
11. Meo PL, D'Anna F, Riela S, Gruttadauria M (2003) Org Biomol Chem 1:1584
12. Agbaria RA, Butterfield MT, Warner IM (1996) J Phys Chem 100:17133
13. Dyck ASM, Kisiel U, Bohne C (2003) J Phys Chem B 107:11652
14. Craig MR, Hutchings MG, Claridge TDW (2001) Angew Chem Int Ed 40:1071
15. Takei M, Yui H, Hirose Y, Sawada T (2001) J Phys Chem A 105:11395
16. Bortolus P, Monti S (1987) J Phys Chem 91:5046
17. Sanchez AM, de Rossi RH (1996) J Org Chem 61:3446
18. Abou-Hamdan A, Bugnon P, Saudan C, Lye PG, Merbach AE (2000) J Am Chem Soc 122:592
19. Harata K (2003) Carbohydr Res 338:353
20. Udachin KA, Wilson LD, Ripmeester JA (2000) J Am Chem Soc 122:12375
21. Kamitori S, Matsuzaka O, Kondo S, Muraoka S, Okuyama K, Nohuchi K, Okada M, Harada A (2000) Macromolecules 33:1500
22. Liu Y, Zhao YL, Zhang HY, Yang EC, Guan XD (2004) J Org Chem 69:3383
23. Fabian J, Hartmann H (1980) Light absorption of organic colorants, in reactivity and structure concepts in orgnic chemistry, vol. 12. Springer, Berlin
24. Mohr GJ, Wolfbeis OS (1994) Anal Chim Acta 292:41
25. Jorgenson MJ, Hartter DA (1963) J Am Chem Soc 85:878
26. Yagil G (1967) J Phys Chem 71:1045
27. Zollinger H (1991) Color chemistry: syntheses, properties and applications of organic dyes and pigments. VCH, Weinheim
28. Joshi H, Kamounah FS, van der Zwan G, Gooijer C, Antonov L (2001) J Chem Soc Perkin Trans 2:2303
29. Antonov L, Fabian WMF, Nedeltcheva D, Kamounah FS (2002) J Chem Soc Perkin Trans 2:1173
30. Antonov L, Stoyanov S, Stoyanova T (1994) Dyes Pigm 26:149
31. Antonov L, Stoyanov S (1995) Dyes Pigm 28:31
32. Smoluch M, Joshi H, Gerssen A, Gooijer C, van der Zwan G (2005) J Phys Chem A 109:535
33. Zhu A, Wang B, White JO, Drickamer HG (2004) J Phys Chem B 108:891
34. Alarcón SH, Olivieri AC, Labadie GR, Cravero RM, Gonzales-Sierra M (1995) Tetrahedron 51:4619
35. Reichardt C, Dimorth K (1968) Fortschr Chem Forsch 11:1
36. Biolet L, Kawaski A (1962) Z Naturforsch 179:621
37. Lippert E (1955) Z Naturforsch 18A:541
38. Rajendiran N, Swaminathan M (1996) Bull Chem Soc Jpn 69:2447
39. Rajendiran N, Swaminathan M (1995) J Photochem Photobiol A Chem 90:109
40. Rajendiran N, Swaminathan M (1996) Indian J Chem 35A:818
41. Hepworth DJ, Mason D, Hallas G, Marsden R (1985) Dyes Pigm 6:389
42. Krishnamoorthy G, Dogra SKJ (1999) Photochem Photobiol A Chem 123:109
43. Kim TH, Cho DW, Yoon M, Kim D (1996) J Phys Chem 160:15670
44. Jiang YB (1995) J Photochem Photobiol A Chem 88:109

45. Agbaria RA, Uzar B, Gill D (1989) J Phys Chem 93:3855
46. Stalin T, Rajendiran N (2006) Chem Phys 322:311
47. Stalin T, Rajendiran N (2006) J Photochem Photobiol A Chem 182:137
48. Stalin T, Rajendiran N (2006) J Photochem Photobiol A Chem 177:144
49. Balasubramanian T, Rajendiran N (2008) Spectrochim Acta 69A:822
50. Antony Muthu Prabhu A, Rajendiran N (2010) Indian J Chem 49A:407
51. Benesi HA, Hildebrand JH (1949) J Am Chem Soc 71:2703
52. Antony Muthu Prabhu A, Siva S, Sankaranarayanan RK, Rajendiran N (2010) J Fluoresc 20:43
53. Kano K, Tawiya Y, Hashimoto S (1992) J Incl Phenom 3:287
54. Tabushi I (1984) Tetrahedron 40:269
55. Guo Q-X, Luo S-H, Liu Y-C (1998) J Incl Phenom Mol Recognit Chem 30:173
56. Li S, Purdy WC (1992) Chem Rev 92:1457
57. Matsui Y, Mochida K (1979) Bull Chem Soc Jpn 52:2808
58. Connors KA, Lin SF, Wong AB (1982) J Pharm Sci 71:217
59. Davies DM, Savage JR (1993) J Chem Res (M):0663
60. Davies DM, Deary ME (1995) J Chem Soc Perkin Trans 2:1287
61. Kitagawa M, Hoshi H, Sakurai M, Inoue Y, Chujo R (1987) Carbohydr Res 163:c1
62. Sakurai M, Kitagawa M, Inoue Y, Chujo R (1990) Carbohydr Res 198:181
63. Delaage M (1991) In: Delaage M (ed) Molecular recognition mechanisms, Ch. 1. VCH Publishers, New York
64. Nemethy G (1967) Angew Chem Int Ed Engl 6:195
65. Sueishi Y, Kasahara M, Inoue M, Matsueda K (2003) J Incl Phenom Macrocycl Chem 4:71
66. Liu Y, Zhao YL, Chen Y, Guo DS (2005) Org Biomol Chem 3:584